Journal of Sound and Vibration (2002) **254**(1), 163–174
doi:10.1006/jsvi.2001.4091, available online at http://www.idealibrary.com on IDEAL®

GLOBAL CHAOS CONTROL OF NON-AUTONOMOUS SYSTEMS

Y.-C. Hsiao and P. C. Tung

Department of Mechanical Engineering, National Central University, Chung-Li, 32054 Taiwan, Republic of China. E-mails: s3312004@cc.ncu.edu.tw; t331166@ncu.edu.tw

(*Received* 12 *December* 2000, *and in final form* 17 *October* 2001)

This study describes a global approach of controlling chaos to reduce tedious waiting time caused by using conventional local controllers. With Euler's method, a non-autonomous system is approximated by a non-linear difference system and then an approximate global Poincaré map function is derived from the difference system by iterating one or more periods of a periodic excitation. Based on the map function, unstable periodic orbits embedded in a chaotic motion can be detected and a global controller for a targeted unstable periodic orbit is designed. The global controller makes all the unstable periodic orbits vanish except a targeted periodic orbit. Furthermore, a Lyapunov's direct method is applied to confirm that the global controller can asymptotically stabilize the unique periodic orbit. For practical applications, system models are usually unknown. To obtain a mathematical model, non-linear system identification based on the harmonic balance principle is applied to an unknown chaotic system of a noisy environment. Simulation results demonstrate that the global controller successfully regularizes a chaotic motion even if the chaotic trajectory is far from the targeted periodic orbit.

1. INTRODUCTION

Recently, chaotic motions of many non-linear systems [1] have received much attention. These motions are trajectories in which infinite unstable periodic orbits (UPOs) are embedded. Chaos is generally undesirable in many fields. This irregular and complex phenomenon erodes system performance and causes fatigue failures [2–4]. Therefore, a lot of methods for regularizing a chaotic motion to an equilibrium point or a periodic orbit have been proposed [5, 6].

Many investigations have concentrated their studies of controlling chaos on autonomous systems in which no forcing inputs are involved [6]. Due to the fact that equilibrium points of autonomous systems are easily determined, strategies are easily designed to control a chaotic response to an equilibrium point [7, 8]. Chen [8] applied a Lyapunov method to design a global controller by letting only an equilibrium point exist in a controlled chaotic system. Meanwhile, many strategies controlled a chaotic response to a periodic orbit of necessity [9, 10]. Some studies have been attempted to regularize chaos to a UPO that is embedded in a chaotic response [11–15]. Such approaches need only a slight amount of control energy. The most popular methods is an approach studied by Ott, Grebogi and Yorke (OGY) [11]. They detected the UPO through the close returns method [16] in a long time series. Next, the OGY controller perturbed on adjustable parameter to stabilize the targeted UPO.

Studies of controlling chaos for non-autonomous systems in which forcing inputs are involved are more limited. Due to the forcing inputs, no strategies successfully control

0022-460X/02/$35.00

a chaotic response to a point of phase space [17], except for impractical approaches which assume that control input can cancel the forcing inputs. Meanwhile, some strategies used high gains to force trajectories of the system to approach the point [18]. However, the trajectories were bounded only around the point. The point was not asymptotically stable. Controlling a chaotic motion to an arbitrary periodic orbit requires additional control energy to suppress the forcing inputs [19, 20] and thus may limit practical applications. Meanwhile, controlling chaos to a UPO embedded in a chaotic motion of a non-autonomous system needs less energy. Some approaches regularized the chaotic motion to the UPO via local dynamics near the UPO [11–14, 21, 22]. Pyragas [14] employed a delay feedback to control the chaotic response to a targeted UPO in phase space. Other strategies controlled the chaotic motions via a Poincaré section that stroboscopically samples a point on a trajectory per period of the UPO. In the latter studies, detection of UPOs on the Poincaré section is simpler that that in phase space because the UPOs correspond to unstable fixed points on the section. The strategies are designed through local dynamics near a targeted UPO on the Poincaré section.

The above approaches of controlling chaos are local since design of the strategies is based on the local dynamics around a targeted UPO that is determined via a long time series. To confirm successful controls, the local controllers were activated only when current states were close to the targeted UPO so that a tedious waiting time was required before activating the controllers. In addition, detection of the UPO took a lot of time. However, for some systems in which chaos may exist, it is necessary to reduce the time in controlling the chaos [23]. Some investigations were enhanced to extend a range in which the controllers can be activated and then reduce the waiting time [24, 25]. However, these controllers are still local, and the constrained ranges limit those improvements.

In this study, a method of shortening the waiting time and detecting the UPOs is proposed by using a function of a global Poincaré map that is a mapping of an intersection point of a trajectory with the Poincaré section onto the subsequent intersection point. A global controller that can be immediately activated to regularize a chaotic motion to a unique UPO is studied. Designing the global controller requires the complete function of the global Poincaré map. However, deriving the exact function is a problem as complicated as that of the solution of the system itself. Identification of the function via a measured time series on the Poincaré section is difficult due to the fractal geometry of strange attractors. Currently, only local map functions about a certain fixed point are obtained through fitting methods [16].

The significance of this study is in developing a general strategy of designing a global chaos control of a non-autonomous system via an approximate global Poincaré map function. A non-linear difference system approximates the non-autonomous system by applying Euler's method [26]. The unknown non-autonomous system of noisy environment is identified via the harmonic balance method [27]. Meanwhile, the approximate global Poincaré map function is derived from the difference system by iterating the difference equation during one or more periods of a periodic excitation. After deriving the approximate map function, UPOs can be detected through the function. Identification of the unknown system requires only a short time series of few periods of the periodic excitation. Thus the UPOs are quickly determined. Based on the function, the global strategy is designed to ensure that a targeted UPO is unique. Next, a Lyapunov's direct method [28] is used to confirm that the designed global strategy can control a chaotic motion asymptotically to the unique UPO. The strategy can be started immediately once the occurrence of chaotic motions is observed and then the chaotic motions can be quickly controlled to a targeted UPO.

2. APPROXIMATE POINCARÉ MAP OF NON-AUTONOMOUS SYSTEMS

The purpose of this study is to globally control a chaotic trajectory of a non-autonomous system to a UPO embedded in the trajectory itself. A controlled chaotic non-autonomous system in which a periodic excitation is involved is illustrated as

$$\dot{\mathbf{x}} = \mathbf{F}(\mathbf{x}, \mathbf{u}, 2\pi ft), \tag{1}$$

where f denotes the frequency of the periodic excitation. The force $\mathbf{u} = \boldsymbol{\eta}(\mathbf{x}, \bar{\mathbf{x}}_d)$ is a feedback control. $\bar{\mathbf{x}}_d$ is a target of the UPOs $\bar{\mathbf{x}}$. No equilibrium points exist in the system due to the excitation [17]. The periods of the UPOs embedded in the chaotic trajectory of the system are multiples of the period of excitation, denoted period-k. To implement conveniently the design of controlling chaos, a Poincaré section that stroboscopically samples a point on a trajectory per period of the UPO is adopted. The Poincaré map of equation (1) is illustrated as

$$\tilde{\mathbf{y}}_{i+1} = \mathbf{G}(\tilde{\mathbf{y}}_i, \tilde{\mathbf{v}}_i), \tag{2}$$

where $\tilde{\mathbf{y}}_i = \mathbf{x}(ikT)$, $\mathbf{v}_i = \boldsymbol{\eta}(\mathbf{x}(ikT), \bar{\mathbf{x}}_d(ikT)) \equiv \boldsymbol{\zeta}(\tilde{\mathbf{y}}_i, \tilde{\mathbf{y}}_d^*)$, $\tilde{\mathbf{y}}_d^* = \bar{\mathbf{x}}_d(ikT)$, and the integers $i \geqslant 0$, $k > 0$. T is the forcing period of the periodic excitation. The Poincaré map $\mathbf{G}$ simplifies the design of the chaos control.

Detecting the UPOs and designing the global control of chaos require the derived function of $\mathbf{G}$. However, deriving the exact Poincaré map is a problem as complicated as that of the solution of the system itself. This study applies Euler's method [26] to overcome the problem. According to the Euler's method, equation (1) is approximated as a difference equation

$$\mathbf{x}_{l+1} = \mathbf{f}(\mathbf{x}_l, \mathbf{u}_l, 2\pi fl\Delta t), \tag{3}$$

where $\mathbf{x}_l = Ax(l\Delta t)$, $\mathbf{u}_l = \mathbf{u}(l\Delta t)$, the integer $l \geqslant 0$, and Δt denotes a time step. The non-singular matrix A is a transformation matrix. The global Poincaré map function is a composite function as given by

$$\mathbf{y}_{i+1} = \mathbf{f}_{J-1} \circ \mathbf{f}_{J-2} \circ \cdots \circ \mathbf{f}_0(\mathbf{x}_{i.J}, \mathbf{u}_{i.J}, 2\pi fi\mathbf{J}\Delta t) \equiv \mathbf{g}(\mathbf{y}_i, \mathbf{v}_i), \tag{4}$$

where $\mathbf{y}_i = \mathbf{x}_l|_{l=i.J}$, $\mathbf{v}_i = \mathbf{u}_l|_{l=i.J} = \boldsymbol{\zeta}(A^{-1}\mathbf{y}_i, A^{-1}\mathbf{y}_d^*) \equiv \boldsymbol{\xi}(\mathbf{y}_i, \mathbf{y}_d^*)$, $\mathbf{y}_d^* = A\tilde{\mathbf{y}}_d^*$, $i, \mathbf{J} \in N$, $i \geqslant 0$, and $\mathbf{J} = kT/\Delta t$. $\mathbf{g}$ is the global map function approximated by the difference equation. Each period kT is divided into $\mathbf{J}$ intervals. The function $\mathbf{f}_\tau$ is the function $\mathbf{f}$ in $l = i\mathbf{J} + \tau$, while the positive integer τ is less than $\mathbf{J}$. The series $\mathbf{y}_i$ is constructed by a part of the series $\mathbf{x}_l$ in $l = 0$, $\mathbf{J}$, $2\mathbf{J}$, … , $i\mathbf{J}$ with an initial condition $\mathbf{x}_0$; that is, the ith element of the series $\mathbf{y}_i$ is the ($i\mathbf{J}$)th element of the series $\mathbf{x}_l$. The approximate function of $\mathbf{G}$ is derived through the function $\mathbf{g}$

$$\mathbf{G}(\tilde{\mathbf{y}}_i, \tilde{\mathbf{v}}_i) \approx A^{-1}\mathbf{g}(A\tilde{\mathbf{y}}_i, \boldsymbol{\xi}(A\tilde{\mathbf{y}}_i, A\tilde{\mathbf{y}}_d^*)) \equiv \hat{\mathbf{G}}(\tilde{\mathbf{y}}_i, \tilde{\mathbf{v}}_i). \tag{5}$$

After deriving the approximate global Poincaré map, the global dynamics of non-autonomous systems can be analyzed.

3. GLOBAL CHAOS CONTROL

The fundamental idea of the global control of chaos is that the strategy stabilizes a targeted UPO of a chaotic non-autonomous system and makes the rest of the UPOs vanish in the same time. Detection of UPOs is necessary to implement the global control. The UPO corresponds to an unstable fixed point $\tilde{\mathbf{y}}^*$ on the Poincaré section and can be

determined through zeros of the equation given below

$$\check{\mathbf{G}}(\tilde{\mathbf{y}}, \tilde{\mathbf{v}}_i) = \hat{\mathbf{G}}(\tilde{\mathbf{y}}, \tilde{\mathbf{v}}_i) - \tilde{\mathbf{y}}. \tag{6}$$

To simplify the analysis via a Lyapunov's direct method [28], this study translates a targeted fixed point $\tilde{\mathbf{y}}_d^*$ to the origin of the co-ordinate. Equation (2) can be approximated as

$$\tilde{\mathbf{z}}_{i+1} \approx \hat{\mathbf{G}}(\tilde{\mathbf{z}}_i + \tilde{\mathbf{y}}_d^*, \tilde{\mathbf{v}}_i) - \mathbf{y}_d^* \equiv \mathbf{H}(\tilde{\mathbf{z}}_i, \tilde{\mathbf{w}}_i), \tag{7}$$

where $\tilde{\mathbf{z}}_i = \tilde{\mathbf{y}}_i - \tilde{\mathbf{y}}_d^*$ and $\tilde{\mathbf{w}}_i = \zeta(\tilde{\mathbf{z}}_i + \tilde{\mathbf{y}}_d^*, \tilde{\mathbf{y}}_d^*) \equiv \phi(\tilde{\mathbf{z}}_i, \tilde{\mathbf{y}}_d^*)$. Based on the approximate global Poincaré maps, one can observe the global dynamics of the controlled chaotic system. The controller changes the dynamic characteristics of the original uncontrolled system and varies the locations of the fixed points of the controlled system. According to the observation, one can design a strategy that preserves the targeted fixed point at the original location and makes the others vanish. In addition, the Lyapunov's direct method is applied to analyze the stability of the targeted fixed point. A Lyapunov function V on the Poincaré section [28] is given as

$$V(\tilde{\mathbf{z}}_i) = \tilde{\mathbf{z}}_i^{\mathrm{T}} Y \tilde{\mathbf{z}}_i, \tag{8}$$

where Y is a symmetric and positive-definite matrix. According to the Lyapunov's direct method, the origin is asymptotically stable if the following difference of the Lyapunov function is negative-definite:

$$\Delta V(\tilde{\mathbf{z}}_i)/\|\tilde{\mathbf{z}}_i\| = (\tilde{\mathbf{z}}_{i+1}^{\mathrm{T}} Y \tilde{\mathbf{z}}_{i+1} - \tilde{\mathbf{z}}_i^{\mathrm{T}} Y \tilde{\mathbf{z}}_i)/\|\tilde{\mathbf{z}}_i\| < -q, \tag{9}$$

where $\tilde{\mathbf{z}}_i \in \mathbf{R}^n - \{0\}$, $q \in \mathbf{R}$, and $q > 0$. According to equation (7), ΔV of equation (9) is approximated as

$$\Delta V(\tilde{\mathbf{z}}_i) \approx \mathbf{H}(\tilde{\mathbf{z}}_i, \tilde{\mathbf{w}}_i)^{\mathrm{T}} Y \mathbf{H}(\tilde{\mathbf{z}}_i, \tilde{\mathbf{w}}_i) - \tilde{\mathbf{z}}_i^{\mathrm{T}} Y \tilde{\mathbf{z}}_i \tag{10}$$

for a specified $\tilde{\mathbf{w}}_i$. The values of ΔV for various $\tilde{\mathbf{z}}_i$ are computed numerically. Because the other fixed points vanish in the proposed strategy, the targeted fixed point is globally stable if the fixed point confirms the Lyapunov's direct method.

4. NUMERICAL EXAMPLE AND DISCUSSION

To illustrate the implications of this study, a controlled Duffing equation in which chaos exists is taken as an example

$$m\ddot{x} + h\dot{x} + \alpha x + \gamma x^3 = p\cos(2\pi f t) + u, \tag{11}$$

where m, h, α, γ, p, f are the non-dimensional parameters of the non-autonomous system and u is the control force. Time t is also non-dimensional. For practical applications, system parameters, including m, h, α, and γ, are unknown. Non-linear system identification based on the harmonic balance principle is applied to evaluate these parameters for $u = 0$ [27]. First, the chaotic output $x(t)$ and the input $p\cos(2\pi f t)$ were simultaneously measured. To simulate experimental measurements, the time series $x(t)$ was perturbed using a 0·15 maximum random noise. Second, an appropriate mathematical model that captures the dynamic characteristics of the physical system was assumed. An appropriate form of polynomial approximated the unknown non-linear terms of the system. Third, the measured input and output of the system were expressed in the Fourier series. Finally,

the expressed terms were substituted into the appropriate mathematical model. By applying the harmonic balance principle, the unknown parameters were determined via a least-squares method [27]. According to the above process, the identified parameters are $m = 0{\cdot}94839$, $h = 0{\cdot}10229$, $\alpha = -0{\cdot}49181$, and $\gamma = 0{\cdot}47997$. Compared to the values of the system parameters in a chaotic region, which are given as $m = 1{\cdot}0$, $h = 0{\cdot}1$, $\alpha = -0{\cdot}5$, $\gamma = 0{\cdot}5$, $p = 0{\cdot}1$, $f = 0{\cdot}125$, respectively, the maximum error of the system identification is below 6% at a noise-to-signal ratio 9·82%.

To derive the approximate global Poincaré map, the Duffing equation was approximated by the appropriate difference function $\mathbf{f}$ of equation (3) that is illustrated as

$$\mathbf{f}(\mathbf{x}_l, \mathbf{u}_l, 2\pi fl\Delta t) = \{x_{l+1}, f_1\}^{\mathrm{T}}, \tag{12}$$

where $\mathbf{x}_l = \{x_1, x_{l+1}\}^{\mathrm{T}}$, $\mathbf{u}_l = \{0, u_l\}^{\mathrm{T}}$, and

$$f_1 = [(2m - h\Delta t)x_{l+1} + (h\Delta t - m - \alpha\Delta t^2)x_l - \gamma\Delta t^2 x_l^3 + p\Delta t^2 \cos(2\pi fl\Delta t) + u_l\Delta t^2]/m.$$

The Poincaré map function $\mathbf{g}$ was derived from equations (4) and (12). The approximate Poincaré map $\hat{\mathbf{G}}$ was derived through equation (5) and the function $\mathbf{g}$. For $\mathbf{u} = 0$, three fixed points $\tilde{\mathbf{y}}^*$ of period-1, $\{-1{\cdot}22581, 0{\cdot}40347\}^{\mathrm{T}}$, $\{-0{\cdot}09264, 0{\cdot}00545\}^{\mathrm{T}}$, and $\{0{\cdot}24433, 0{\cdot}12642\}^{\mathrm{T}}$ were detected by solving zeros of equation (6). After selecting a targeted fixed point $\tilde{\mathbf{y}}_d^* = \{-0{\cdot}09264, 0{\cdot}00545\}^{\mathrm{T}}$, equation (7) was derived through equations (4), (5), and (12). Meanwhile, by transformation of co-ordinates, the three fixed points were translated by $\{-1{\cdot}13317, 0{\cdot}39802\}^{\mathrm{T}}$, $\{0{\cdot}0, 0{\cdot}0\}^{\mathrm{T}}$ and $\{0{\cdot}33697, 0{\cdot}12098\}^{\mathrm{T}}$ respectively.

The next work is to determine the form of the control. To simplify the description, this study selected a strategy of controlling chaos,

$$\mathbf{u} = k_\alpha(x - \bar{x}_{d,1}), \tag{13}$$

where $\bar{x}_{d,1}$ is the first element of the vector $\bar{\mathbf{x}}_d$. The study selected the control gain as 0·6 to preserve the origin and make other fixed points vanish. Meanwhile, the designed global strategy would stabilize the unique fixed point. The origin is asymptotically stable if the matrix

$$Y = \begin{bmatrix} 1 & 0 \\ 0 & c^2 \end{bmatrix} \tag{14}$$

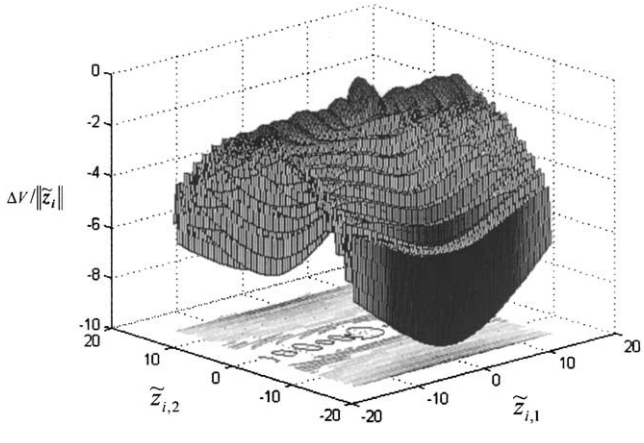

Figure 1. Values of $\Delta V/\|\tilde{\mathbf{z}}_i\|$ in the region $\{\tilde{\mathbf{z}}_i = \{\tilde{z}_{i,1}, \tilde{z}_{i,2}\}^{\mathrm{T}} | -15 \leqslant \tilde{z}_{i,1} \leqslant 15, \quad -15 \leqslant \tilde{z}_{i,2} \leqslant 15\} - \{0\}$. $m = 0{\cdot}94839$, $c = 0{\cdot}10229$, $\alpha = -0{\cdot}49181$, $\gamma = 0{\cdot}47997$, $p = 1$, $f = 0{\cdot}125$, $k_\alpha = 0{\cdot}6$, and $\Delta t = 0{\cdot}0016$.

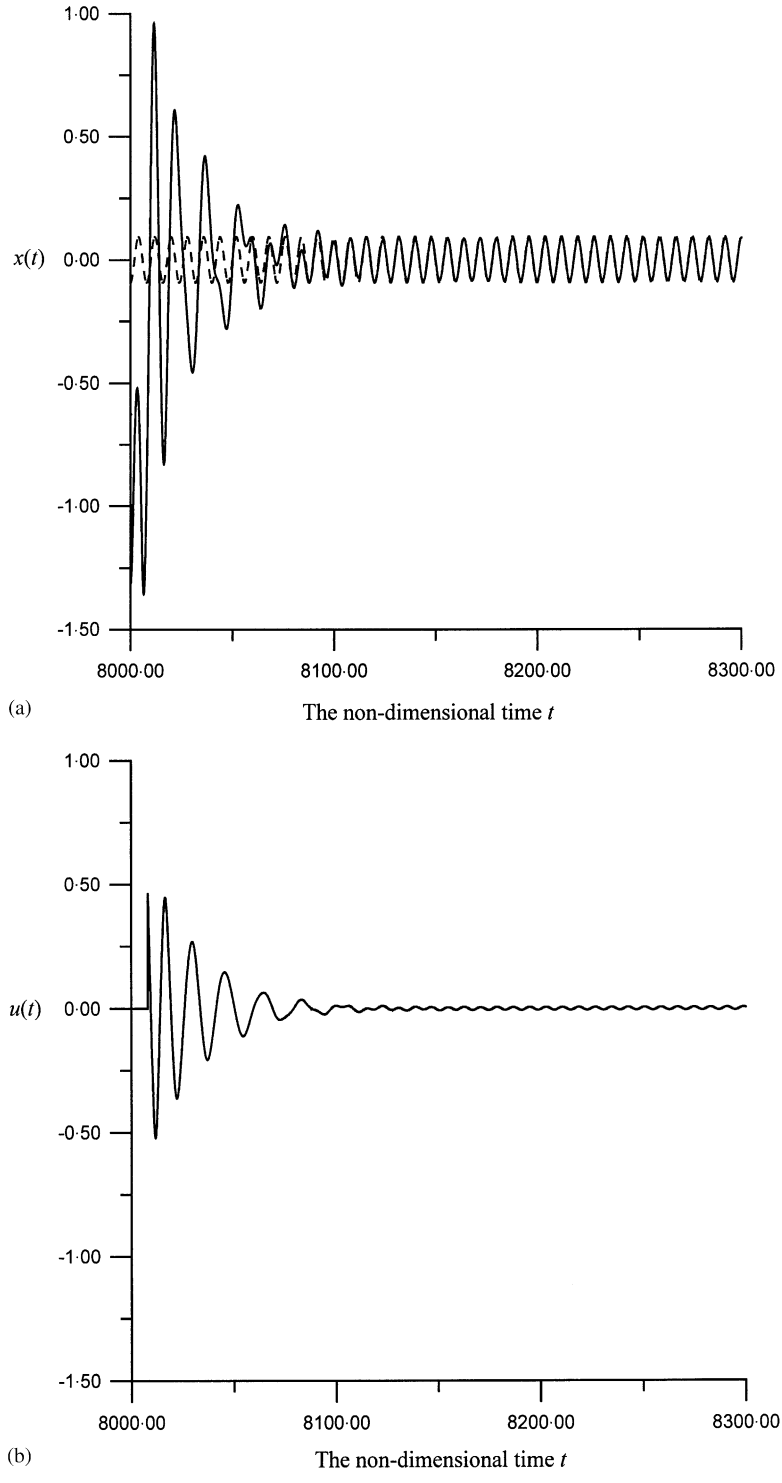

Figure 2. (a). Time response of the controlled Duffing equation in the control process of $k_\alpha = 0{\cdot}6$. ——, shows the output $x(t)$; ....., denotes the targeted UPO. (b) The control force $u(t)$ in the control process. $m = 1{\cdot}0$, $h = 0{\cdot}1$, $\alpha = -0{\cdot}5$, $\gamma = 0{\cdot}5$, $p = 1$, $f = 0{\cdot}125$, $\tilde{\mathbf{y}}_d^* = \{-0{\cdot}09264, 0{\cdot}00545\}^{\mathrm{T}}$.

results in the negative-definite $\Delta V/\|\tilde{\mathbf{z}}_i\|$, where $\tilde{\mathbf{z}}_i = \{\tilde{z}_i, \tilde{z}_{i+1}\}^{\mathrm{T}}$. The constant c serves to unify the vector field of the Duffing equation. Figure 1 illustrates that the origin is asymptotically stable because all the values of $\Delta V/\|\tilde{\mathbf{z}}_i\|$ are negative-definite in the region $\{\tilde{\mathbf{z}}_i | -15 \leqslant \tilde{z}_i \leqslant 15, \ -15 \leqslant \tilde{z}_{i+1} \leqslant 15\} - \{0\}$.

To verify the proposed strategy, this study applied the strategy to control the chaotic Duffing equation. Figure 2(a) presents the time response of equation (11) with the proposed global strategy. The controller was activated at the non-dimensional time 8008. Figure 2(b) shows the control force during the control process. After the beginning of the control, the chaotic motion soon approached the targeted periodic orbit after the non-dimensional time 8216. Simultaneously, the absolute value of the control energy declined to below 0·006. The little non-zero control energy results from the error of detecting the targeted UPO. This study selected a small value of k_α as possible because a large control gain amplifies the detection error and then enlarges control errors. Furthermore, in comparison to another controller, an OGY control was designed according to the same identified system parameters and the same targeted UPO. The OGY controller was as effective as the proposed controller at the non-dimensional time 8008, and then was activated at the non-dimensional time 14248 when the maximum variation of α is 0·6. Compared to the global control, the OGY controller must wait 781 periods of the periodic excitation to be activated. The global control had stabilized the targeted UPO far before the OGY controller being activated because the control does not need to wait for the chaotic trajectory to approach the targeted UPO. For the globally controlling chaos, the controlled system does not need to bear constantly the chaotic motion of large vibration.

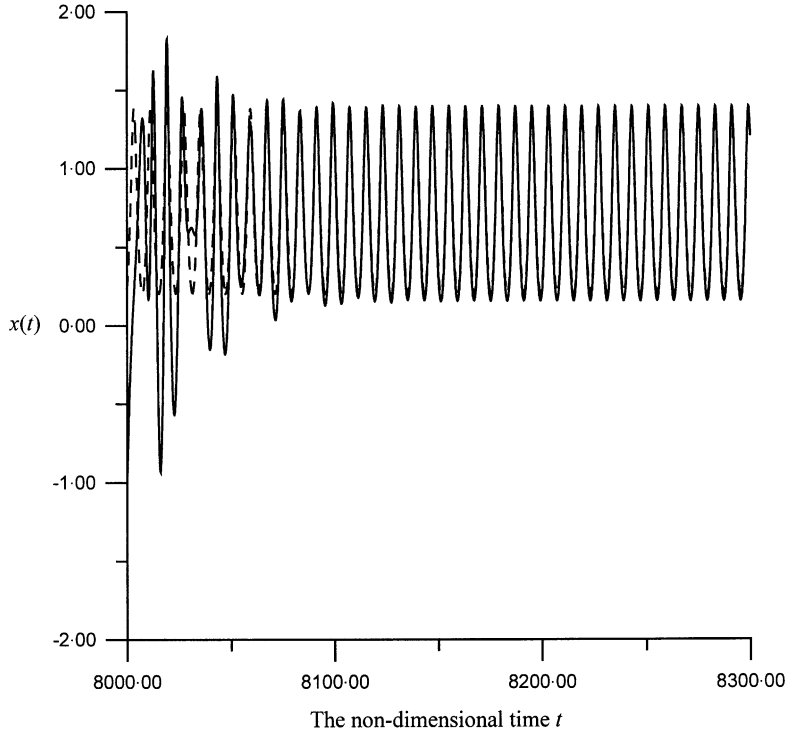

Figure 3. Time response of the controlled Duffing equation in the control process of $k_\alpha = 0{\cdot}8$. ——, shows the output $x(t)$; ....., denotes the targeted UPO. $m = 1{\cdot}0$, $h = 0{\cdot}1$, $\alpha = -0{\cdot}5$, $\gamma = 0{\cdot}5$, $p = 1$, $f = 0{\cdot}125$, $\tilde{\mathbf{y}}_d^* = \{0{\cdot}24433, 0{\cdot}12642\}^{\mathrm{T}}$.

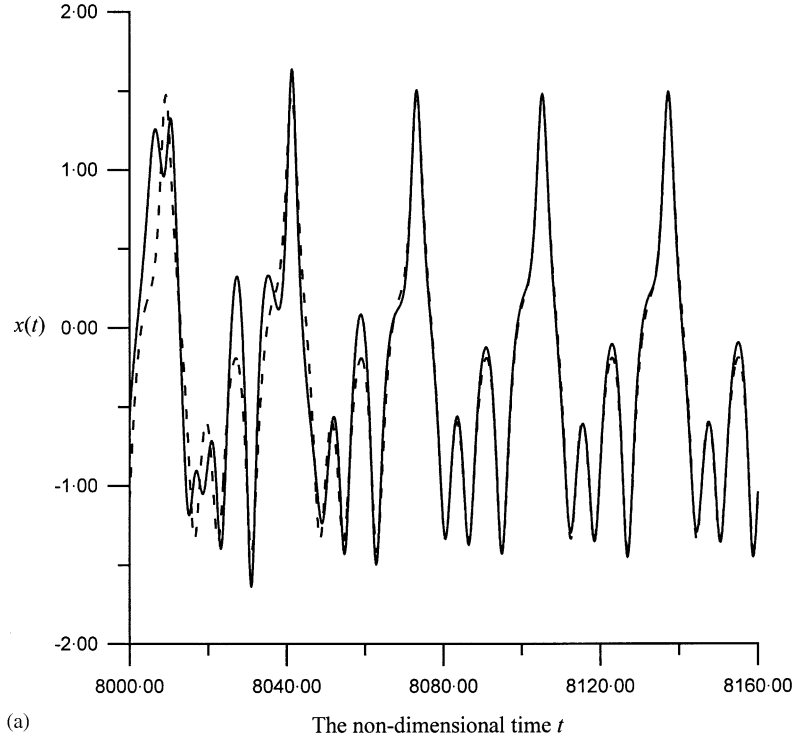

(a)

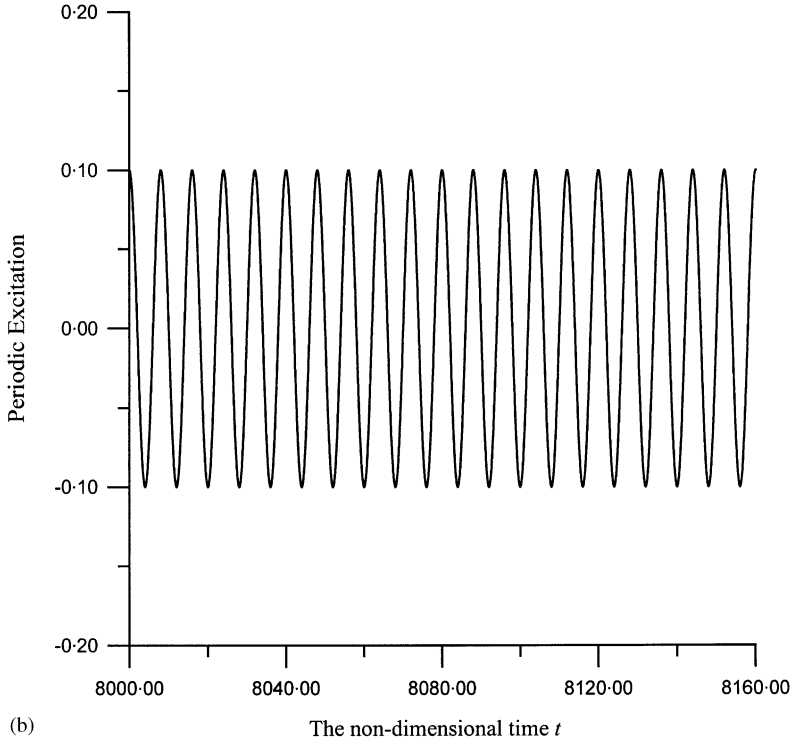

(b)

Figure 4. (a). Time response of the controlled system illustrated in equation (15) in the control process of $k_\alpha = 0{\cdot}8$. ——, shows the output $x(t)$; ....., denotes the targeted UPO. (b) The periodic excitation of the system. $m = 1{\cdot}0$, $h = 0{\cdot}1$, $\alpha = -0{\cdot}5$, $\gamma = 0{\cdot}5$, $p = 1$, $f = 0{\cdot}125$, $\tilde{\mathbf{y}}_d^* = \{-1{\cdot}08864, 0{\cdot}52062\}^{\mathrm{T}}$.

It should be noted that the control can stabilize another UPO. For example, the strategy globally stabilized another unstable fixed points of period-1 $\tilde{\mathbf{y}}^* = \{0{\cdot}24433, 0{\cdot}12642\}^{\mathrm{T}}$ by selecting the point as the targeted fixed point and designing the control gain as 0·8. Figure 3 displaces the time response of equation (11) with the designed control. The controller was activated at the non-dimensional time 8008. In addition, the proposed approach works when the method is applied to stabilize a UPO of a high period. Figure 4(a) describes that the proposed strategy globally controls the chaotic motion to an unstable fixed point of period-4 $\{-1{\cdot}08864, 0{\cdot}52062\}^{\mathrm{T}}$ by selecting the fixed point as the target and designing the control gain as 0·8. The controller was activated at the non-dimensional time 8008. The period of the stabilized fixed point is clearly observed by comparing the time responses in Figure 4(a) with the periodic excitation portrayed in Figure 4(b).

To increase the persuasion of the global control of chaos, the proposed approach is applied to another chaotic system described in the following:

$$m\ddot{x} + h\dot{x} + \alpha x + N(x) = p\cos(2\pi ft) + u, \tag{15}$$

where $m = 1$, $h = 0{\cdot}04$, $a = 1$, $p = 4{\cdot}26$, $f = 0{\cdot}125$, and u is a control force. The function of $N(x)$ is presented as follows:

$$N(x) = \begin{cases} 0, & |x| < 0{\cdot}5, \\ 15\,[x - 0{\cdot}5\,\mathrm{sign}(x)], & |x| \geqslant 0{\cdot}5, \end{cases} \tag{16}$$

where $\mathrm{sign}(x)$ denotes the signum function of x. In practical application, the exact model of the system is unknown. To implement the global control of chaos, an approximate mathematical non-linear model with $u \equiv 0$ and unknown non-linear terms that is approximated by a truncated polynomial of $x(t)$ is assumed as follows:

$$\tilde{m}\ddot{x} + \tilde{h}\dot{x} + \tilde{\alpha}x + N_p(x) = p\cos(2\pi ft), \tag{17}$$

where $N_p(x) = \sum_{j=2}^{14} \gamma_j x^j$. According to the process of the non-linear system identification described above, the identified parameters of the approximate model are evaluated and

TABLE 1

Results of system identification for equation (17)

Parameters of the approximate model	Identified values
$\tilde{m}$	0·992
$\tilde{h}$	0·038
$\tilde{\alpha}$	1·067
γ_2	1·496
γ_3	− 17·2
γ_4	− 8·437
γ_5	118·9
γ_6	19·82
γ_7	− 201
γ_8	− 24·56
γ_9	157·1
γ_{10}	17·03
γ_{11}	− 59·03
γ_{12}	− 6·226
γ_{13}	8·605
γ_{14}	0·923

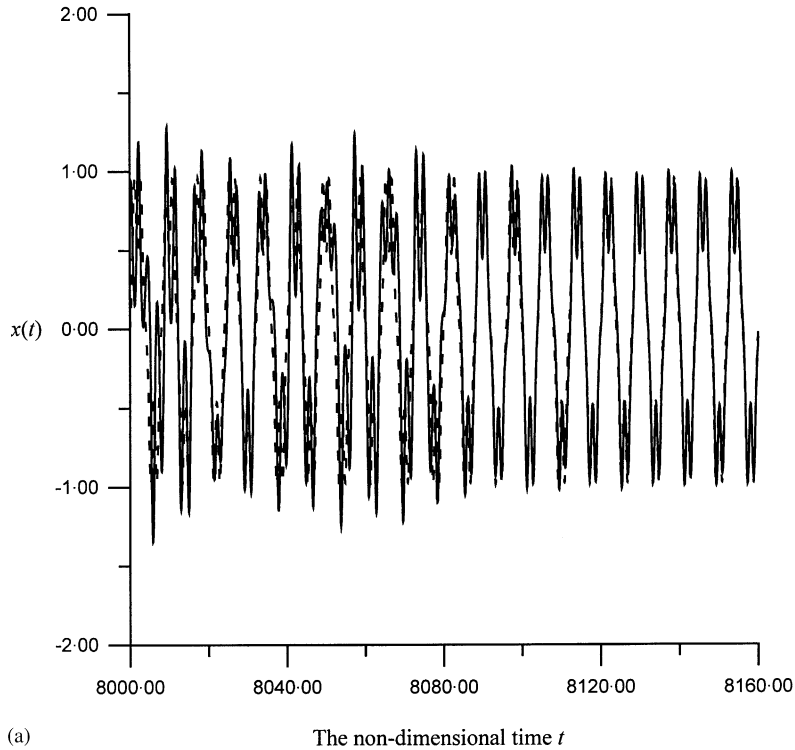

(a)

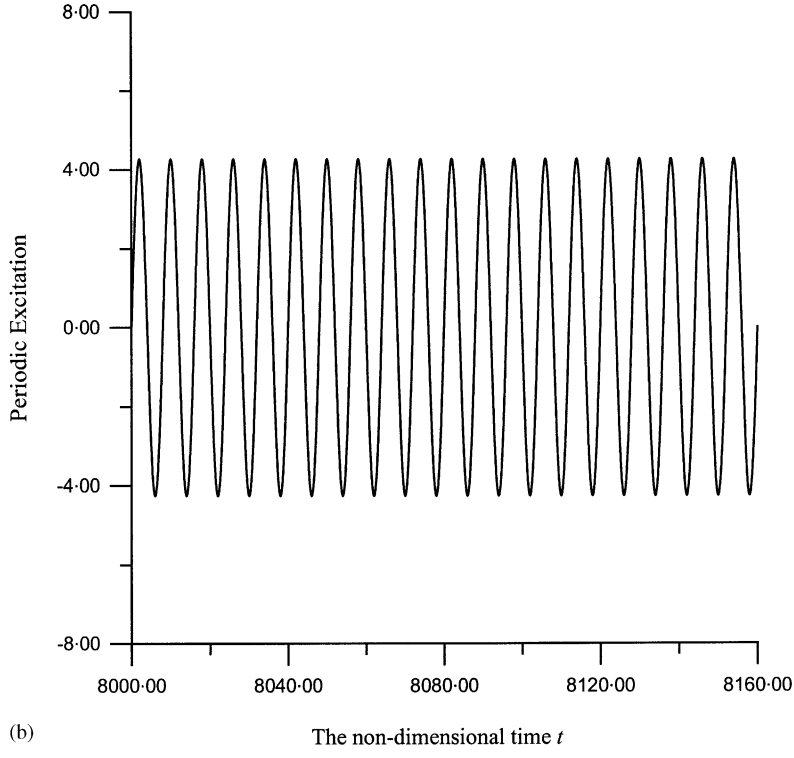

(b)

Figure 5. (a). Time response of the controlled system illustrated in equation (15) with the control process of $k_\alpha = -1{\cdot}2$. ——, shows the output $x(t)$; ....., denotes the targeted UPO. (b) The periodic excitation of the system. $m = 1$, $h = 0{\cdot}04$, $\alpha = 1$, $p = 4{\cdot}26$, $f = 0{\cdot}125$, $\tilde{\mathbf{y}}_d^* = \{-0{\cdot}00601, 0{\cdot}45740\}^T$.

described in Table 1. An unstable fixed point of period-1 $\{-0{\cdot}00601, 0{\cdot}45740\}^{\mathrm{T}}$ is detected based on the approximate model and then is selected as the targeted fixed point. Meanwhile, a strategy of controlling chaos is selected as the description in equation (13) and applied to the system illustrated in equation (15). Figure 5(a) shows the time response of equation (15) by designing the control gain as $-1{\cdot}2$. The controller was activated at the non-dimensional time 8008. The proposed strategy globally stabilized the targeted unstable fixed point. The period of the stabilized UPO is observed according to Figures 5(a) and 5(b).

5. CONCLUSIONS

This study has designed a global controller that controlled a chaotic trajectory to a targeted UPO in a non-autonomous system. The proposed global controller, which does not require waiting time in activating the controller, can be rapidly started to stabilize the targeted UPO. Meanwhile, the Lyapunov's direct method confirmed that the targeted periodic orbit is globally asymptotically stable. In addition, it should be noted that the differential system can be obtained by the system identification that requires only a short chaotic time series in which noise is present since a chaotic motion contains broadband of frequencies. The proposed approach is simple and can shorten the times both in detecting UPOs and in controlling chaos.

The proposed global controller is benefited from the approximate global Poincaré map. Thus one can study global dynamics of non-autonomous systems without local limitation based on the approximate global Poincaré map. In addition, it should be noted that not only the proposed P control is suitable to the global strategy but also, all kinds of appropriated controllers can be applied to the strategy based on the obtained global Poincaré map.

REFERENCES

1. T. Kapitaniak 1992 *Chaotic Oscillators—Theory and Applications*. Singapore: World Scientific.
2. D. R. Chialvo, R. F. Gilmour Jr and J. Jalife 1990 *Nature* **343**, 653–657. Low dimensional chaos in cardiac tissue.
3. Z.-M. Ge and H.-H. Chen 1998 *Journal of Sound and Vibration* **209**, 753–769. Double degeneracy and chaos in a rate gyro with feedback control.
4. Z.-M. Ge, H.-S. Yang, H.-H. Chen and H.-K. Chen 1999 *International Journal of Engineering Science* **37**, 921–943. Regular and chaotic dynamics of a rotational machine with a centrifugal governor.
5. G. Chen and X. Dong 1998 *From Chaos to Order—Methodologies, Perspectives and Applications*. Singapore: World Scientific.
6. E. Ott, T. Sauer and J. A. Yorke 1994 *Coping with Chaos—Analysis of Chaotic Data and the Exploitation of Chaotic Systems*. New York: John Wiley & Sons.
7. T. T. Hartley and F. Mossayebi 1992 *International Journal of Bifurcation and Chaos* **2**, 881–887. A classical approach to controlling the Lorenz equations.
8. Y. H. Chen and M. Y. Chou 1994 *Physical Review E* **50**, 2331–2334. Continuous feedback approach for controlling chaos.
9. S. J. Schiff, K. Jerger, D. H. Duong, T. Chang, M. L. Spano and W. L. Ditto 1994 *Nature* **370**, 615–620. Controlling chaos in the brain.
10. J. Alvarez-Ramírez 1994 *Physical Review E* **50**, 2339–2342. Nonlinear feedback for controlling the Lorenz equation.
11. E. Ott, C. Grebogi and J. A. Yorke 1990 *Physical Review Letters* **64**, 1196–1199. Controlling chaos.
12. W. L. Ditto, S. N. Rauseo and M. L. Spano 1990 *Physical Review Letters* **65**, 3211–3214. Experimental control of chaos.

13. E. R. HUNT 1991 *Physical Review Letters* **67**, 1953–1955. Stabilizing high-period orbits in a chaotic system: the diode resonator.
14. K. PYRAGAS 1992 *Physics Letters A* **170**, 421–428. Continuous control of chaos by self-controlling feedback.
15. C.-C. FUH and P.-C. TUNG 1995 *Physical Review Letters* **75**, 2952–2955. Controlling chaos using differential geometric method.
16. T. SHINBROT, C. GREBOGI, E. OTT and J. A. YORKE 1993 *Nature* **363**, 411–417. Using small perturbations to control chaos.
17. H. K. KHALIL 1996 *Nonlinear Systems*. Upper Saddle River: Prentice-Hall, second edition.
18. H.-J. SHIEH and K.-K. SHYU 1999 *IEEE Transactions on Industrial Electronics* **46**, 380–389. Nonlinear sliding-mode torque control with adaptive backstepping approach for induction motor drive.
19. H. NIJMEIJER and H. BERGHUIS 1995 *IEEE Transactions on Circuits and Systems—I: Fundamental Theory and Applications* **42**, 473–477. On Lyapunov control of the Duffing equation.
20. G. CHEN and X. DONG 1993 *International Journal of Bifurcation and Chaos* **3**, 1363–1409. From chaos to order—perspectives and methodologies in controlling chaotic nonlinear dynamical systems.
21. Z.-M. GE, C.-I. LEE, H.-H CHEN and S.-C. LEE 1998 *Journal of Sound and Vibration* **217**, 807–825. Non-linear dynamics and chaos control of a damped satellite with partially-filled liquid.
22. Z.-M. GE and T.-N. LIN 2000 *Journal of Sound and Vibration* **230**, 1045–1068. Regular and chaotic dynamic analysis and control of chaos of an elliptical pendulum on a vibrating basement.
23. A. GARFINKEL, M. L. SPANO, W. L. DITTO and J. N. WEISS 1992 *Science* **257**, 1230–1235. Controlling cardiac chaos.
24. E. BARRETO, E. J. KOSTELICH, C. GREBOGI, E. OTT and J. A. YORKE 1995 *Physical Review E* **51**, 4169–4172. Efficient switching between controlled unstable periodic orbits in higher dimensional chaotic systems.
25. K. YAGASAKI and T. UOZUMI 1998 *Physics Letters A* **238**, 349–357. A new approach for controlling chaotic dynamical systems.
26. P. G. REINHALL, T. K. CAUGHEY and D. W. STORTI 1989 *Transactions of the American Society of Mechanical Engineers, Journal of Applied Mechanics* **56**, 162–167. Order and chaos in a discrete Duffing oscillator: implications on numerical integration.
27. K. YASUDA, S. KAWAMURA and K. WATANABE 1988 *JSME International Journal, Series III—Vibration, Control Engineering and Engineering or Industry* **31**, 8–14. Identification of nonlinear multi-degree-of-freedom systems (presentation of an identification technique).
28. Y. TAKAHASHI, M. J. RABINS and D. M. AUSLANDER 1970 *Control*. Reading, Massachusetts: Addison-Wesley.